BB

Invited paper presented at International Symposium on
Muon Catalyzed Fusion (μCF95), Dubna, June 19–24,

TRI–PP–95–92
Dec 1995

Muon Catalyzed Fusion in Deuterium at 3 K

P.E. Knowles[1], J.M. Bailey[2], G.A. Beer[1], J.L. Beveridge[3],
M.C. Fujiwara[4], T.M. Huber[5], R. Jacot–Guillarmod[6], P. Kammel[7],
S.K. Kim[8], A.R. Kunselman[9], G.M. Marshall[3], C.J. Martoff[10], G.R. Mason[1],
F. Mulhauser[3,*], A. Olin[3], C. Petitjean[11], T.A. Porcelli[1] and J. Zmeskal[12]

[1] *University of Victoria, Victoria, British Columbia, V8W 2Y2 Canada*

[2] *Chester Technology, England*

[3] *TRIUMF, Vancouver, British Columbia, V6T 2A3 Canada*

[4] *University of British Columbia, Vancouver, British Columbia, V6T 2A6 Canada*

[5] *Gustavus Adolphus College, St. Peter, MN 56082, USA*

[6] *Université de Fribourg, CH-1700 Fribourg, Switzerland*

[7] *LBL, Berkeley, CA 94720, USA*

[8] *Jeonbuk National University, Jeonju City 560–756, S. Korea*

[9] *University of Wyoming, Laramie, WY 82071, USA*

[10] *Temple University, Philadelphia, PA 19122, USA*

[11] *Paul Scherrer Institute, CH-5232 Villigen, Switzerland*

[12] *Austrian Academy of Sciences, A-1090 Wien, Austria*

Muon catalyzed fusion in deuterium has traditionally been studied in gaseous and liquid targets. The TRIUMF solid hydrogen layer target system has been used to study the fusion reaction rates in the solid phase at a target temperature of 3 K. Both branches of the cycle were observed; neutrons by a liquid organic scintillator, and protons by a silicon detector located inside the target system. The effective molecular formation rate from the upper hyperfine state and the spin exchange rate have been measured, and information on the branching ratio parameters has been extracted.

Keywords: muon catalyzed fusion, deuterium, solid.

1 Introduction

During the commissioning of the TRIUMF layered solid hydrogen target system, data were taken on μCF in solid deuterium. The preliminary values for the kinetics parameters

*Present address: Université de Fribourg, CH-1700 Fribourg, Switzerland

were in sharp disagreement with theory and have initiated further investigations of the reactions in solid [1, 2].

2 Experimental Setup

The target system used in this measurement has been presented elsewhere [3, 4]. Layers of solid deuterium, each 10.54(53)mg·cm^{-2} thick and ~40 cm^2 in area, were frozen onto 50.4 μm thick gold foils maintained at 3 K. Because a palladium filter at 600 K was used to purify the D_2 gas immediately prior to freezing, the ratio of even to odd molecular spins was expected to be statistical (nD_2)[5].

Muons entered the target by passing through the thin gold layer, which acted as a degrader, and stopped either in the first or second solid hydrogen layer. Muon catalyzed fusion of dμd molecules then occurred. The higher energy fusion products, neutrons at 2.45 MeV and protons at 3.02 MeV, were detected.

The arrangement of detectors has been given in [3] with the modification that two neutron detectors were used. Each neutron detector was a 12.5 cm diameter by 10 cm deep cylinder of NE–213 liquid scintillator viewed by a photomultiplier. Pulse shape discrimination (PSD) was used to differentiate between photon and neutron events. An event veto based on anticoincidence with charged–particle detectors ensured that only events from neutral particles were gated to the PSD units. These veto scintillators were also used as electron detectors to record the electron following muon decay.

A silicon detector of 600 mm^2 active area was mounted inside the vacuum system and viewed the solid deuterium layer directly. Its 150 μm active thickness was sufficient to measure protons of up to 4.5 MeV, and was well suited for detecting the fusion protons at 3.02 MeV.

The timing of all events was taken with respect to the time of the incident muon as measured by a beam entrance scintillator.

Measurements with pure solid layers of D_2 and $^1H_2$ were made at TRIUMF in August of 1992. The thick D_2 layers received an integrated muon flux of 220 × 10^6 μ with (57.6±1.3)% stopped in the solid layers, while the study of the background in $^1H_2$ was done with 130 × 10^6 μ, with stopping fractions varying from 30 to 60% depending on the layer thickness used.

3 Reaction Kinetics

The kinetics of the muon catalyzed reactions in pure deuterium have been discussed in [6, 7]. The differential equation representing the kinetics was solved analytically and the solution used for the analysis.

The reduced rate of formation of dμd molecules from a μd atom in the hyperfine state F, $\tilde{\lambda}_F$, is composed via the formula

$$\tilde{\lambda}_F = \lambda_{nr} + \sum_S \lambda_{FS} \frac{\tilde{\lambda}_f}{\tilde{\lambda}_f + \sum_{F'} \Gamma_{SF'}}. \quad (1)$$

It represents molecular formation that leads to fusion and is composed of the nonresonant formation rate and the fraction of resonantly formed molecules which successfully fuse via $\tilde{\lambda}_f$ rather than resonantly scatter as characterized by $\Gamma_{SF'}$ (back decay)[7]. Likewise, the reduced hyperfine transition rate from state F to F', $\tilde{\lambda}_{FF'}$, has contributions from regular scattering and from the decay of the resonance dμd complex:

$$\tilde{\lambda}_{FF'} = \lambda_{FF'} + \sum_{S} \lambda_{FS} \frac{\Gamma_{SF'}}{\tilde{\lambda}_f + \sum_{F''} \Gamma_{SF''}}. \tag{2}$$

The branching ratios for the two hyperfine states, β_F, will differ due to the distribution of angular momentum bound states generated by the different molecular formation processes. The nonresonant formation will lead to both s and p wave bound states of the dμd while resonance formation always produces the p wave molecular state. The β_F's are composed of the s and p wave branching ratios, along with the ratio of s to p wave bound state formation P_s[6, 8]:

$$\beta_F = \frac{\lambda_{nr}}{\tilde{\lambda}_F} \left[P_s \beta_s + (1 - P_s) \beta_p \right] + \frac{\tilde{\lambda}_F - \lambda_{nr}}{\tilde{\lambda}_F} \beta_p. \tag{3}$$

4 Spectra

Neutron events were selected using hardware pulse shape discrimination to suppress the majority of photon events, and a further software PSD cut which was set to maximize the n/γ ratio. A coincidence condition requiring that the muon survives until after the neutron event, enforced by observing the muon decay time with respect to the neutron, was necessary to enhance the fusion signal with respect to the strong neutron background from nuclear muon capture.

The time spectrum with a delayed electron coincidence condition, as well as the time spectrum of the capture neutrons accidentally gated into the coincidence spectrum, are shown in Fig. 1. The constant neutron flux present in the experimental hall also generated events which passed the coincidence cut, and its contribution is shown as well. Kinetics parameters were extracted from a fit to the data with correction terms for the background.

Protons generated by fusion were detected by the silicon detector. The thickness of the deuterium layer, and the angle between the layer and the detector meant that the proton spectrum was very spread out in energy. Two energy windows were selected, the first in the signal region and the second well above the fusion signal to give a good measure of the background. The signal region energy cut was chosen to favour protons produced inside the layer rather than at its surface to reduce any effect from muon loss by μd emission into the vacuum.

Time spectra for the two energy windows were made for both deuterium and protium layers. From comparisons with the protium layer data, the time dependent scaling of the background between the high energy and low energy cuts was determined. Figure 2 shows the time spectra of the signal and background for the deuterium.

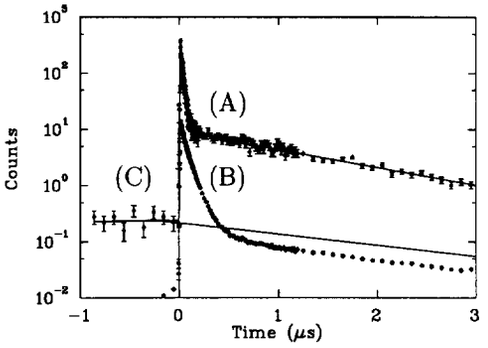

Figure 1: The time spectra for the neutron coincidence spectra (A). The accidentally accepted capture neutrons (B), and the contribution from the constant background (C) are shown.

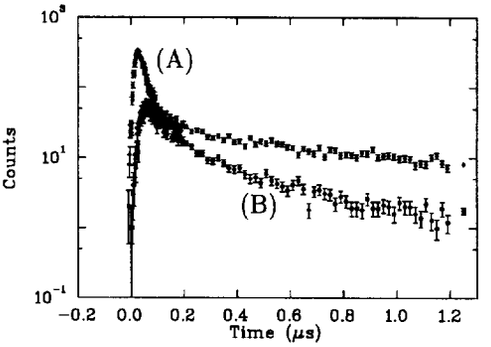

Figure 2: The time spectra from the silicon detector. Curve (A) represents the data containing the fusion proton signal. Curve (B) shows the background.

5 Fit Parameters

The time spectrum function was convoluted with a gaussian resolution function to model the finite time resolution of the detectors, as well as with a step function which turned on the distribution with the muon arrival. Excluding background parameterization, six independent parameters were required to completely determine the shape of a spectrum: two lifetimes, two amplitudes, the detector timing resolution, and the muon arrival time. Since an absolute measurement was not done, one of the parameters in the fit was used for normalization, so only three kinetics parameters could be extracted from a single time spectrum. By fitting the time spectra of both the neutron and proton data simultaneously, four kinetics parameters could be extracted (equivalent to doing an absolute measurement for a single fusion product spectrum). It was necessary to use one parameter to fit the small nitrogen contamination of the target.

The fits to the spectra are sensitive to the values of $\tilde{\lambda}_{\frac{3}{2}\frac{1}{2}}$, $\tilde{\lambda}_{\frac{3}{2}}$, $\phi_z\lambda_z$ (the loss rate to nitrogen), and one of $\tilde{\lambda}_{\frac{1}{2}}$, P_s, β_s, or β_p. Thus the four extracted parameters are dependent on the input values of the remaining three. The standard values of the parameters passed to the fitting routine are given in Table 1. The fits gave a χ^2 value of 325 for 309 degrees of freedom. Within the quoted errors, variations in ϕ and ω_s did not cause meaningful variations in the fitted parameters.

With $\tilde{\lambda}_{\frac{1}{2}}$ and any two of P_s, β_s, and β_p fixed, the resulting values of the physical parameters are:

$$\tilde{\lambda}_{\frac{3}{2}} = 2.71(7)_{stat.}(32)_{sys.}\ \mu s^{-1}$$
$$\tilde{\lambda}_{\frac{3}{2}\frac{1}{2}} = 34.2(8)_{stat.}(1)_{sys.}\ \mu s^{-1}$$
$$\phi_z\lambda_z = 0.320(10)_{stat.}(1)_{sys.}\ \mu s^{-1}$$
$$\beta_p = 0.563(14)_{stat.}(11)_{sys.}$$
$$\beta_s = 0.487(15)_{stat.}(11)_{sys.}$$
$$P_s = 0.47(8)_{stat.}(6)_{sys.}.$$

Table 1
Table of standard values passed to the fitting routine.

Parameter	Value	Source
ω_s	0.122(3)	Experiment: Balin *et al.* [9]
ϕ	1.4269(4)	Experiment: Petitjean *et al.* [10]
$\tilde{\lambda}_{\frac{1}{2}\frac{3}{2}}$	0 μs^{-1}	Detailed balance of $\tilde{\lambda}_{\frac{3}{2}\frac{1}{2}}$ at 3 K
$\tilde{\lambda}_{\frac{1}{2}}$	0.044(5) μs^{-1}	Experiment: Scrinzi *et al.* [11]
P_s	0.560	Theory: Faĭfman [8]
β_s	0.470	Theory: Hale [12]
β_p	0.580(5)	Experiment: Zmeskal *et al.* [6]

The fit values of $\tilde{\lambda}_{\frac{3}{2}\frac{1}{2}}$, $\tilde{\lambda}_{\frac{3}{2}}$, and $\phi_z\lambda_z$ do not change when each of P_s, β_s, and β_p is varied with the remaining two parameters fixed at the standard values. This behaviour is expected from Eq. (3) which enters the kinetics as a distinct subformula. The large systematic uncertainty in the $\tilde{\lambda}_{\frac{3}{2}}$ value is due almost entirely to the uncertainty in the $\tilde{\lambda}_{\frac{1}{2}}$ input value.

Setting all three of P_s, β_s, β_p to the standard values allowed a measurement of $\tilde{\lambda}_{\frac{1}{2}}$, resulting in:

$$\tilde{\lambda}_{\frac{1}{2}} = 0.052(8)_{stat.}(3)_{sys.}\ \mu s^{-1},$$
$$\tilde{\lambda}_{\frac{3}{2}} = 3.21(51)_{stat.}(16)_{sys.}\ \mu s^{-1},$$
$$\tilde{\lambda}_{\frac{3}{2}\frac{1}{2}} = 34.0(8)_{stat.}(1)_{sys.}\ \mu s^{-1},$$
$$\phi_z\lambda_z = 0.320(10)_{stat.}(1)_{sys.}\ \mu s^{-1}.$$

The systematic uncertainty in this case is dominated by the variations in the β_p value.

Plots of the values for $\tilde{\lambda}_{\frac{3}{2}}(T)$ and $\tilde{\lambda}_{\frac{3}{2}\frac{1}{2}}(T)$ from other work, including the theoretically predicted values, are shown in Figs. 3 and 4.

6 Discussion

The value found for $\tilde{\lambda}_{\frac{3}{2}\frac{1}{2}}$ is consistent with the direct scattering rate as calculated in [13], but the considerable theoretical difficulties in reproducing the measured $\tilde{\lambda}_{\frac{3}{2}\frac{1}{2}}$ rate for the gas and liquid experiments allow no simple conclusions to be drawn from this experiment in solid.

The high value of $\tilde{\lambda}_{\frac{3}{2}}$, about two orders of magnitude larger than the expected formation rate for thermalized μd in D_2 at 3 K, can be interpretated as an indication of solid state effects. Two possible effects are discussed here.

The scattering of μd in solid D_2 has been calculated and there are large differences for low energy scattering when compared to scattering from free molecules [18]. When the collision of the μd occurs at energies high above the binding energy of a D_2 in the lattice, the collision will proceed as if the D_2 were free. As the energy of successive collisions is reduced, the μd will begin to scatter from the entire crystal, and the huge mass of the lattice will make it difficult for the μd to lose lab energy in elastic collisions. In addition, there are no available phonon modes to allow inelastic scattering for μd with a few meV

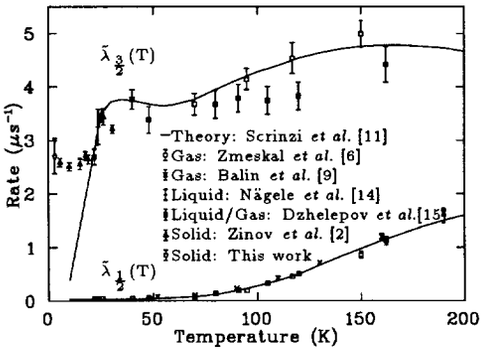

Figure 3: A graph of molecular formation rates measured in solid, liquid and gas, and calculated for liquid and gas. The points of Zinov *et al.* do not include the systematic uncertainty associated with the $\tilde{\lambda}_{\frac{1}{2}}$ value.

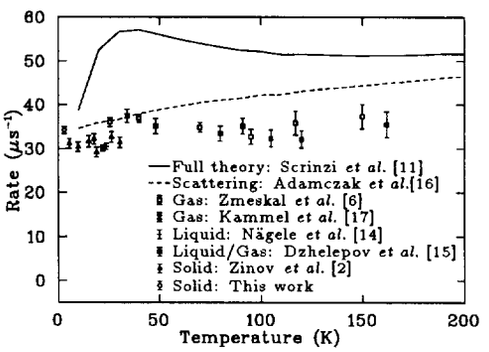

Figure 4: The comparison of $\tilde{\lambda}_{\frac{3}{2}\frac{1}{2}}$ to previously measured values.

energy, and so the energy loss mechanisms for the μd are suppressed when the muonic atoms reach an equivalent energy of about 30 K. Since the molecular formation rate is still resonant in that region, a slow thermalization could account for some of the large rate.

An examination of Eq. (1) shows that an increase in the de-excitation rate leading to fusion, $\tilde{\lambda}_f$, for the resonantly formed $[(d\mu d)^s_{J\nu}\, dee]$ will increase the effective formation rate by more successfully competing with the $\Gamma_{SF'}$ deexcitation mode (back decay). If there exists a sufficiently strong coupling of the ro–vibrational modes of the resonant six–body complex to the phonons in the solid, then there may be sufficient augmentation of the deexcitation rate to allow this effect. The molecular formation rate in solid has not yet been examined for solid state effects, although work on another possible phonon effect has begun [19].

The kinetics model is simple in the sense that time–independent rates are used, an assumption which can be challenged when the thermalization of the μd_F is slow. Since the $\mu d_{\frac{1}{2}}$ are nonresonant for all energy distributions up to about 50 K, the assumption of the time–independent nonresonant rate is valid. For the $\mu d_{\frac{3}{2}}$, a slow thermalization will mean that the average energy distribution changes at a rate similar to an eigenvalue of the problem. Hence the $\tilde{\lambda}_{\frac{3}{2}}$ value would be time dependent and not constant as assumed in the kinetics. Similar problems with kinetics equations and slow thermalizations have been dealt with in [20].

Emission of the μd from the layer is a loss mechanism that is not explicitly taken into account in the analysis, however the process would mimic the $\phi_z\lambda_z$ loss mechanism. The value found for $\phi_z\lambda_z$, coupled with the value for the transfer to nitrogen, $\lambda_z \approx 10^5 \mu s^{-1}$, implies a nitrogen contamination of about 1.5 ppm, a value which was independently measured for the thick deuterium target [21]. If the value were to represent only μd escape from the layer, then roughly one third of all the μd's are emitted from the layer. Given the current understanding of the scattering cross sections [13, 18], this process is unlikely to give such a strong effect. Monte Carlo studies of the dynamic processes are

underway.

Zinov *et al.* [2] have presented values for μCF in solid deuterium over a range of temperatures. That experiment and this one are consistent, however the disagreement with theory indicates that comprehensive calculations for the molecular formation rate including solid state effects must be made. If the even–odd populations of D_2 angular momenta are as important as suggested in [19] then further experiments will be required.

Acknowledgements

The authors wish to thank the funding agencies of NSERC in Canada, DOE in the United States, and the Swiss National Science Foundation.

References

[1] P. Kammel, in *Muonic Atoms and Molecules*, edited by L. A. Schaller and C. Petitjean (Birkhäuser Verlag, CH-4010, Basel, 1993), pp. 111–128, [Proceedings of the Centro Stefano Franscini, Ascona].
[2] V. G. Zinov *et al.*, Measurement of spin and temperature dependence of $dd\mu$ molecule formation rate in gaseous, liquid, and solid deuterium, Proceedings of μCF–95, Dubna, Russia, 1995.
[3] P. E. Knowles *et al.*, Hyp. Int. **82**, 521 (1993).
[4] P. E. Knowles *et al.*, A windowless frozen hydrogen target system, to be published in Nucl. Instrum. Methods.
[5] P. C. Souers, *Hydrogen Properties for Fusion Energy* (University of California Press, Berkeley, California, 1986).
[6] J. Zmeskal *et al.*, Phys. Rev. A **42**, 1165 (1990).
[7] L. I. Man'shikov *et al.*, Zh. Eksp. Teor. Fiz. **92**, 1173 (1987), [Sov. Phys. JETP, **65**(4), 656–663 (1987)].
[8] M. P. Faĭfman, Muon Catal. Fusion **4**, 341 (1989).
[9] D. V. Balin *et al.*, Phys. Lett. B **141**, 173 (1984).
[10] C. Petitjean *et al.*, Muon Catal. Fusion **2**, 37 (1988).
[11] A. Scrinzi *et al.*, Phys. Rev. A **47**, 4691 (1993).
[12] G. M. Hale, Muon Catal. Fusion **5/6**, 227 (1990/91).
[13] A. Adamczak and V. S. Melezhik, Muon Catal. Fusion **4**, 303 (1989).
[14] N. Nägele *et al.*, Nucl. Phys. A **493**, 397 (1989).
[15] V. P. Dzhelepov *et al.*, Zh. Eksp. Teor. Fiz. **101**, 1105 (1992), [Sov. Phys. JETP, **74**(4), 589–595 (1992)].
[16] A. Adamczak, Muon Catal. Fusion **4**, 31 (1989).
[17] P. Kammel *et al.*, Phys. Lett. B **112**, 319 (1982).
[18] A. Adamczak, Thermalization of muonic hydrogen in hydrogen targets, Proceedings of μCF–95, Dubna, Russia, 1995.
[19] L. I. Men'shikov, Proceedings of μCF–95, Dubna, Russia, 1995.
[20] P. Kammel *et al.*, Muon Catal. Fusion **3**, 483 (1988).
[21] R. Jacot-Guillarmod, (private communication).